Microstructure and Nonlinear Properties of Microwave-Sintered ZnO–V$_2$O$_5$ Varistors: I, Effect of V$_2$O$_5$ Doping

Cheng-Tzu Kuo, Chang-Shun Chen,[‡] and I-Nan Lin[‡]

Institute of Materials Science and Engineering, National Chiao-Tung University, Hsinchu,
Taiwan 300, Republic of China

The modification of the densification behavior and the grain-growth characteristics of the microwave-sintered ZnO materials, caused by the incorporation of V$_2$O$_5$ additives, have been systematically studied. Generally, the addition of V$_2$O$_5$ markedly enhances the densification rate, such that a density as high as 97.9% of the theoretical density and a grain size as large as 10 μm can be attained for a sintering temperature as low as 800°C and a soaking time as short as 10 min. Increasing the sintering temperature or soaking time does not significantly change the sintered density of the ZnO–V$_2$O$_5$ materials but it does monotonously increase their grain size. Varying the proportion of V$_2$O$_5$ in the range of 0.2–1.0 mol% does not pronouncedly modify such behavior. The leakage current density (J_L) of these high-density and uniform-granular-structure samples is still large, which is amended by the incorporation of 0.3 mol% of Mn$_3$O$_4$ in the ZnO materials, in addition to 0.5 mol% of the V$_2$O$_5$ additives. Samples that are obtained using such a method possess good nonohmic characteristics (α = 23.5) and a low leakage current density (J_L = 2.4 × 10^{-6} A/cm^2).

I. Introduction

ZINC OXIDE (ZnO) ceramics with several additives are used as varistor materials, because of their highly nonohmic behavior in current–voltage (*I–V*) characteristics and excellent capability of withstanding surges.[1–4] Therefore, these ZnO-based varistors are extensively used as transient surge suppressers against dangerous abnormal high-voltage surges, to protect electronic circuits.[5–8] It is believed that the nonlinear *I–V* characteristics of these materials resulted from the grain-boundary layer, which is essentially formed by a segregation of large ionic additives such as Bi$_2$O$_3$, Pr$_6$O$_{11}$, and BaO, at the grain boundary.[9–13] These ''varistor-forming'' ingredients affect the electrical properties and the densification behavior and microstructure evolution of ZnO ceramics.

Recently, it was reported that V$_2$O$_5$ is another varistor-forming ingredient for ZnO ceramics;[14–16] use of this material results in varistor properties that are similar to those of ZnO–Bi$_2$O$_3$ ceramics. The advantage of the ZnO–V$_2$O$_5$ system is that the ceramics can be sintered at relatively low temperature (i.e., ~900°C) in a conventional electrical furnace. This property is important for applications of multilayer chip components, because the material can be cofired with a silver inner

electrode with a melting point of ~961°C. It is expected that the densification behavior can be further improved by using the microwave sintering technique, because it is generally accepted that this process can densify the ceramic materials at a very rapid rate and at a substantially lower temperature.[17–20]

In this paper, we have made an extensive examination on the effect of sintering temperature and soaking time on the densification behavior of ceramics based on the ZnO–V$_2$O$_5$ system. The correlation between the microstructural characteristics of the materials with their electric properties is discussed.

II. Experimental Procedure

High-purity (>99.9%) ZnO varistor powders, ~0.8 μm in size, were used in the preparations of the ZnO–*x*-mol%-V$_2$O$_5$ materials (*x* = 0–1.0). The mixtures with proper compositions were ball-milled in a plastic jar for 8 h, using zirconia balls and deionized water. After the mixtures were filtered and dried, they were calcined at 700°C in air for 2 h, followed by pulverization in a ball mill for 8 h to a size of ~1.0 μm and then uniaxially pressed at 750 kgf/cm^2 into a disk that was 8 mm in diameter and 2 mm thick. The zirconia contamination was determined, using an inductively coupled plasma (ICP) analyzer, to be <300 ppm. The green pellets, ~60% of the theoretical density (5.675 g/cm^3), were microwave-sintered at 800°–1200°C for 5–60 min in air, using a 2.45 GHz microwave generated from a commercial source (Model GL107 magnetron, Gerling Co., Modesto, CA). The samples were also sin-
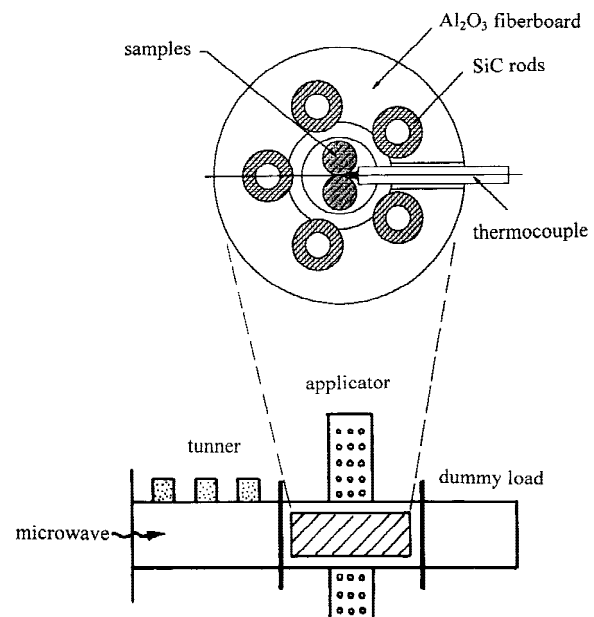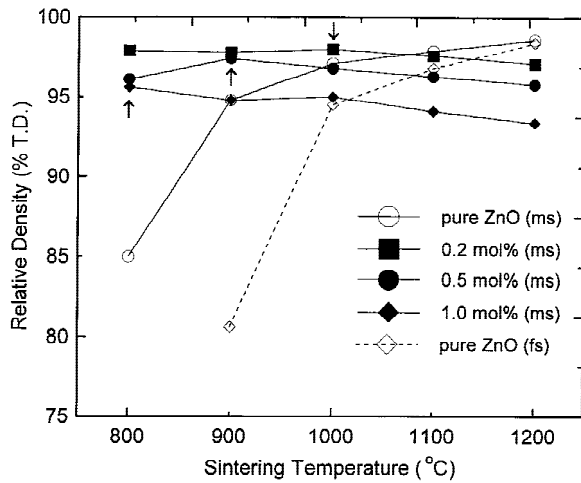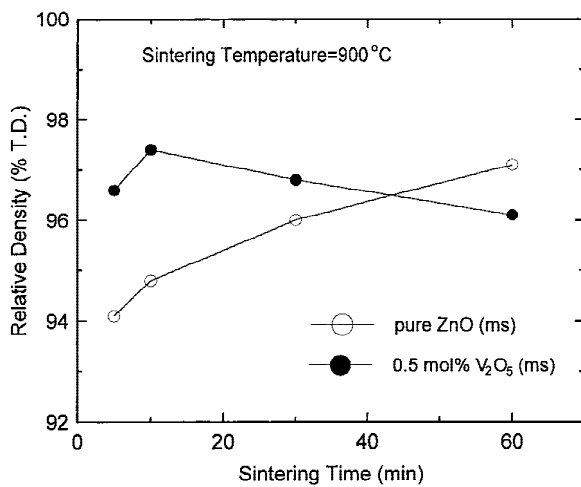

Fig. 1. Schematic drawings of the setup for microwave sintering of ZnO materials.
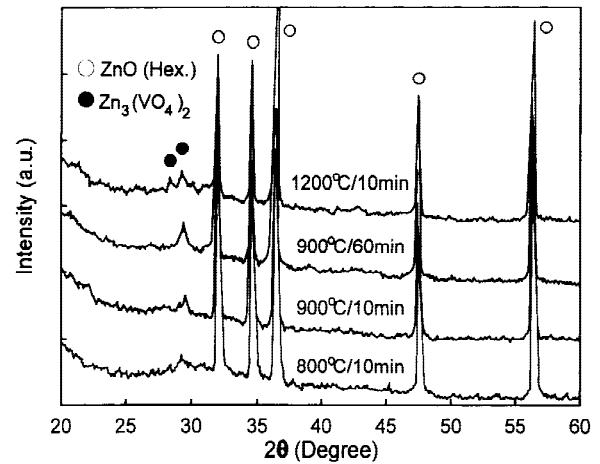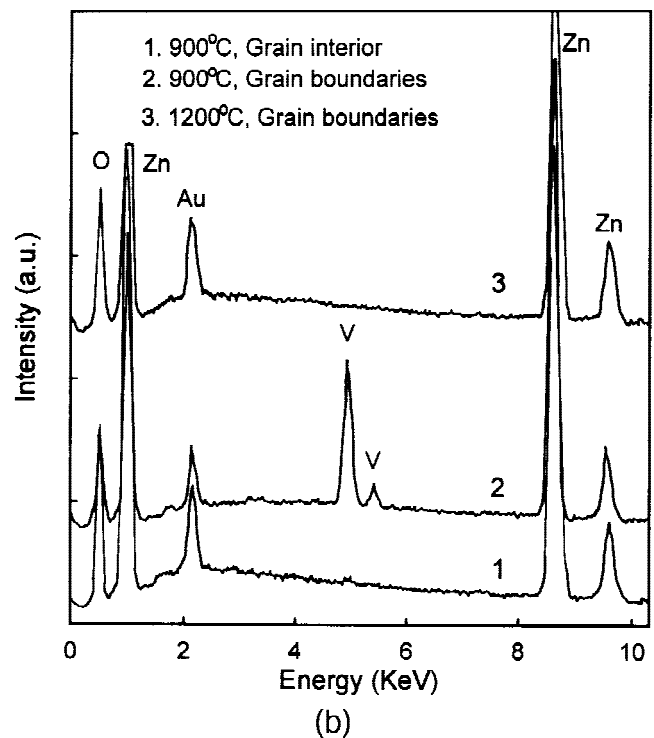
(a)

(a)

(b)

Fig. 2. Densification behavior of ZnO–V$_2$O$_5$ materials ((a) micro-wave-sintered at 800°–1200°C for 10 min (solid curves) or furnace-sintered at 900°–1200°C for 60 min (dotted curve) and (b) microwave-sintered at 900°C for 5–60 min).

(b)

Fig. 3. (a) XRD patterns (Cu*K*α) of ZnO–0.5-mol%-V$_2$O$_5$ materials microwave-sintered at 800°–1200°C for 10 min and (b) EDAX patterns of the surface of ZnO–0.5-mol%-V$_2$O$_5$ materials samples microwave-sintered either at 900°C (pattern 1, grain interior; pattern 2, grain boundaries) or at 1200°C (pattern 3, grain boundaries).

tered at 900°–1200°C for 60 min in an electrical furnace to facilitate the comparison. The heating and cooling rates each were 5°C/min.

In the microwave sintering process, the applicator is a segment of a WR284 waveguide (Gerling), schematically shown in Fig. 1, in which a crucible cut from Al$_2$O$_3$ fiberboard is inserted. The Al$_2$O$_3$ fiberboard was selected to reduce the microwave absorption. SiC rods were used as microwave absorption susceptors to preheat the samples to ~600°C, because the ZnO pellets can only start to absorb microwave and self-generate the heat at that temperature. The temperature profile was measured using a Pt–13% Rh thermocouple that was placed near the sample surface. The thermocouple, which is shielded, should be oriented perpendicular to the electric field in the waveguide, to minimize the disturbance on the micro-wave and to avoid the arcing caused by the pickup of the electric field. The heating rate was controlled at 60°C/min, and the cooling rate was controlled at 145°C/min for sintering temperatures >500°C. The sintering temperature was controlled by adjusting the input microwave power level. The accuracy of the temperature measurement was confirmed by running a test process, in which TiO$_2$ (anatase) samples were heated to ~890°–910°C. The proportion of phase transformation from anatase to the rutile structure was then compared to the materials that

were heat-treated in an electrical furnace. The temperature measurement was determined to have an accuracy of ±10°C in the setup schematically shown in Fig. 1.

The crystal structure and microstructure of the sintering samples were examined using X-ray diffractometry (XRD) (Model XD-5, Shinadzu Co., Kyoto, Japan) and scanning electron microscopy (SEM) (Model JSM-840A, JEOL, Tokyo, Japan), respectively. The density of the sintered specimens was measured by using the Archimedes method. The average grain size, $\overline{G}$, was calculated as described by Mendelson[21] with a multiple factor of 1.56. The *I–V* properties of these samples were measured by using an electrometer (Model 237 I-V, Keithley Instruments, Cleveland, OH) in a dc source after the indium–gallium (40:60) alloy was rubbed onto the sample surface to serve as electrodes. The onset electric field (E_0) was defined as the *E*-values at a current density of 1.0 mA/cm^2, and
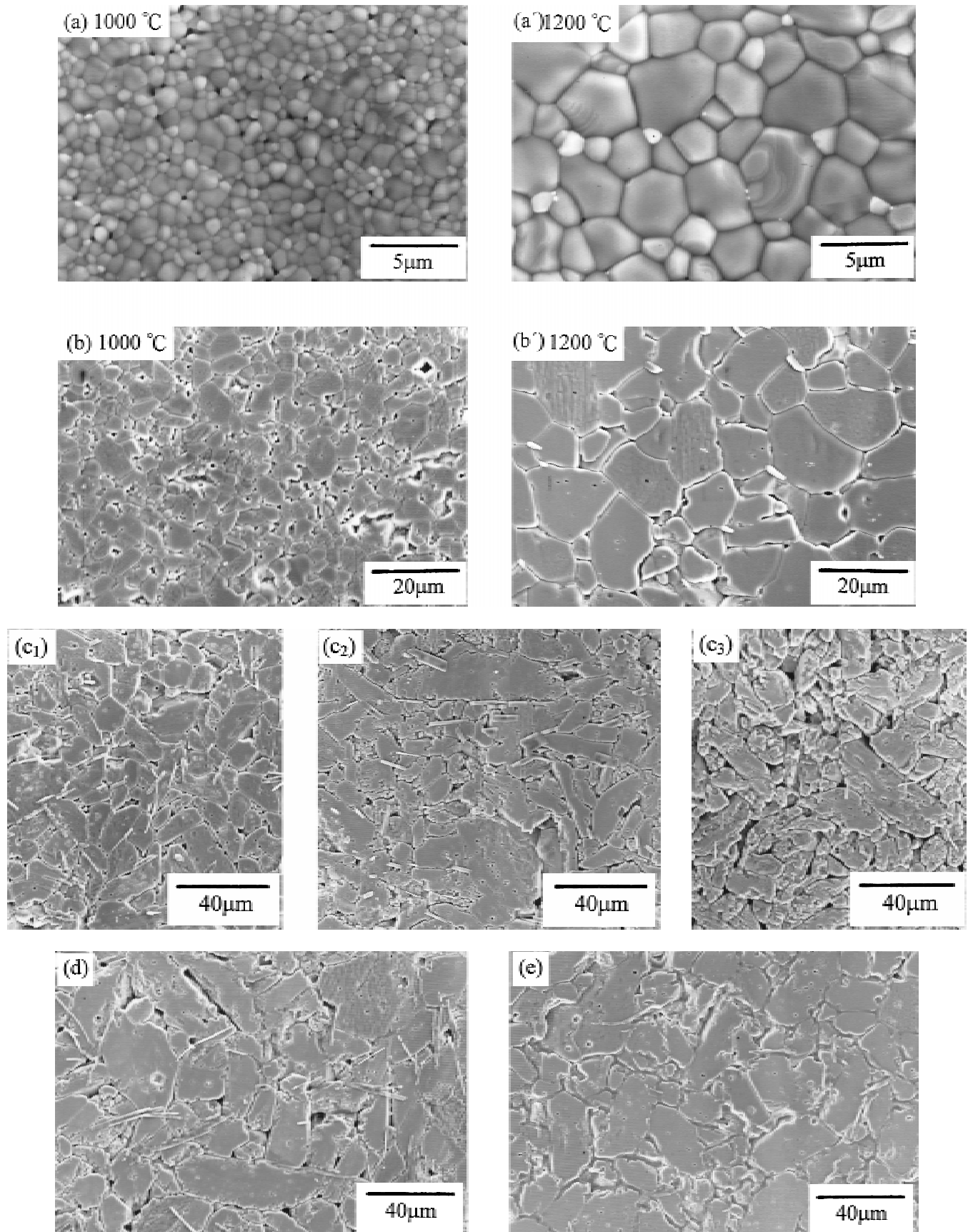
Fig. 4. SEM micrographs of (a and a′) the pure ZnO materials densified via the conventional furnace sintering process at 1000° or 1200°C, respectively, for 60 min; (b and b′) the pure ZnO materials densified via the microwave sintering process at 1000° or 1200°C, respectively, for 10 min; (c₁–c₃) ZnO–0.2-mol%-V_2O_5, ZnO–0.5-mol%-V_2O_5, and ZnO–1.0-mol%-V_2O_5 materials, respectively, densified via the microwave sintering process at 900°C for 10 min; (d) ZnO–0.5-mol%-V_2O_5 material densified via the microwave sintering process at 900°C for 60 min; and (e) ZnO–0.5-mol%-V_2O_5 material densified via the microwave sintering process at 1000°C for 10 min.
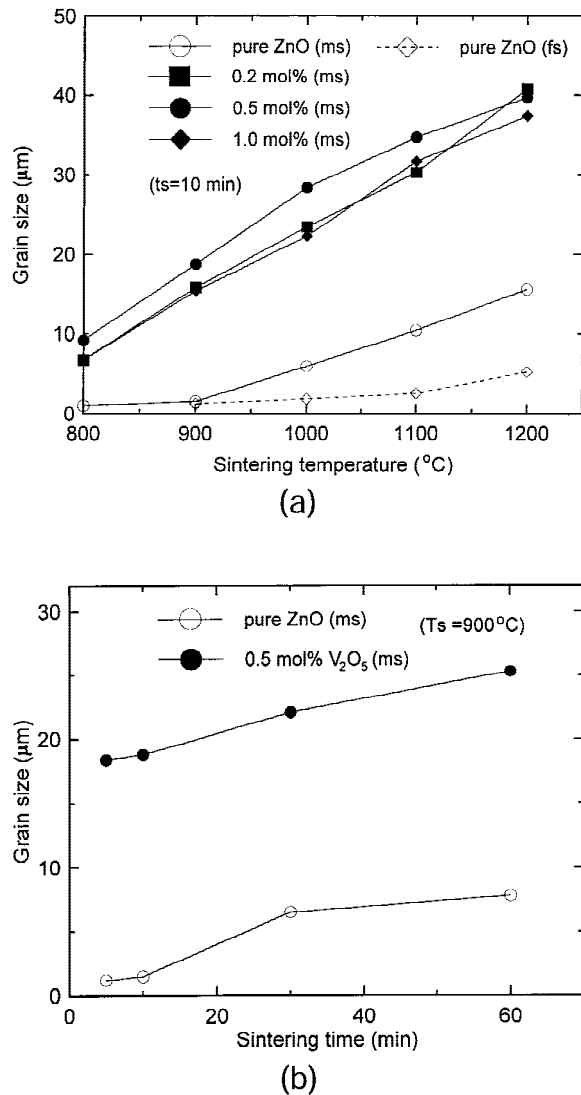
(a)

(b)

Fig. 5. Variation of the grain size of the ZnO–V$_2$O$_5$ materials with (a) sintering temperature (microwave-sintered ("ms") for 10 min or furnace-sintered ("fs") for 60 min) and (b) soaking period (microwave-sintered at 900°C).

the leakage current density (J_L) was defined as the J-values at $E–J$ curves of 10 V/mm. The capacitance–voltage ($C–V$) measurements were made at room temperature using a capacitance meter (Model HP4274A, Hewlett–Packard, Tokyo, Japan). The electrical characteristics, including barrier height (Φ_b) and the donor density (N_d), were determined from $C–V$ data, using the model proposed by Mukae *et al.*[22]

III. Results and Discussion

(1) Sintering Behavior

The beneficial effect of V$_2$O$_5$ on the sintering of the ZnO ceramics is shown in Fig. 2. The open circles in this figure show that, without the V$_2$O$_5$ additives, the ZnO materials can attain sufficient density (i.e., 94.8% of the theoretical density (TD)) only when they are microwave-sintered at a temperature of >900°C for 10 min. The addition of only 0.2 mol% of V$_2$O$_5$ markedly enhances the densification rate, such that the samples attain a density as high as 97.9% of TD when microwave-sintered at 800°C for 10 min (shown as solid squares in Fig. 2(a)). The samples are hardly densified for sintering temperatures <800°C. A density reversion phenomenon—i.e., the de-

crease in density with increasing sintering temperature (T_s)—occurs for $T_s \geq 1000°C$ (marked by arrows). Similar phenomena are observed for ZnO materials that contain either 0.5 mol% or 1.0 mol% V$_2$O$_5$ (shown as solid circles and solid diamonds, respectively, in Fig. 2(a)). The sintered density of ZnO materials is slightly lower for the samples that contain a larger proportion of V$_2$O$_5$. The temperature of density reversion occurs at 900°C for ZnO–0.5-mol%-V$_2$O$_5$ materials and 800°C for ZnO–1.0-mol%-V$_2$O$_5$ materials (marked by arrows in Fig. 2(a)). For comparison, the densification behavior of pure ZnO materials sintered via the conventional furnace heating process is shown as a dotted line in Fig. 2(a), to indicate that this material requires a higher sintering temperature (i.e., >1000°C) and longer soaking time (i.e., 60 min) to attain a density as high as 94.5% of TD. The advantage of the microwave sintering process over the conventional furnace heating process is clearly demonstrated.

The fact that the V$_2$O$_5$ addition can enhance the sintering behavior of the ZnO materials is further demonstrated by the evolution of the density of the samples with the soaking time. As shown in Fig. 2(b), the density of the pure ZnO materials increases monotonously as the soaking period increases, attaining a density of 97.1% of TD when it is microwave-sintered at 900°C for 60 min. However, the ZnO–V$_2$O$_5$ materials already attain a high density (97.4% of TD) when they are microwave-sintered at 900°C for 10 min, and the density of the samples decreases slightly as the soaking time increases thereafter. In other words, the inclusion of V$_2$O$_5$ into ZnO materials markedly enhances the densification rate of these materials; however, the density of the samples decreases when the microwave-sintering temperature is too high or soak time is too long.

To understand how the V$_2$O$_5$ modifies the densification of ZnO materials, the phase constituents of the microwave-sintered ZnO–V$_2$O$_5$ materials have been examined. The XRD patterns in Fig. 3(a) show that the microwave-sintered materials consist of a Zn$_3$(VO$_4$)$_2$ secondary phase, in addition to the hexagonal ZnO phase, whereas the energy-dispersive X-ray analyses (EDAX) via SEM on the as-sintered sample surface (patterns 1 and 2 in Fig. 3(b)) show that the vanadium species are mainly located at grain-boundary regions. These results infer that the V$_2$O$_5$ enhances the densification of the ZnO materials via the mechanism of a liquid-phase sintering process. The liquid phase is, presumably, the eutectic phase between ZnO and Zn$_3$(VO$_4$)$_2$. Moreover, EDAX analyses on the 1200°C microwave-sintered ZnO materials show that no vanadium species are observable in the grain-boundary regions (pattern 3 in Fig. 3(b)), which clearly indicates the loss of the vanadium species when the sintering temperature is too high. Therefore, the density reversion observed in Figs. 2(a) and (b) can be ascribed to the loss of the volatile vanadium species. This observation agrees with the phenomenon that the density reversion of the high-V$_2$O$_5$-containing materials (i.e., ZnO–1.0 mol% V$_2$O$_5$) occurs at a lower temperature than that for the ZnO–0.5-mol%-V$_2$O$_5$ or ZnO–0.2-mol%-V$_2$O$_5$ materials.

The microwave sintering process increases the densification behavior of ZnO materials and enhances the grain-growth rate of the materials. Figures 4(a) and (a′) and Figs. 4(b) and (b′) show materials that were formed via conventional furnace sintering (fs) and microwave sintering (ms) processes, respectively; these grains of pure ZnO materials have grown monotonously as the sintering temperature increases. The grain-growth rate of the ms samples is markedly larger than that of the fs samples, shown as open circles and open diamonds, respectively, in Fig. 5(a). The average grain size of the ms samples sintered at 1200°C (10 min), which is ~12 μm, is markedly larger than that of the fs samples sintered at 1200°C (60 min), which is only ~4 μm.

The addition of the V$_2$O$_5$ species enhances grain growth even more markedly; however, the proportion of V$_2$O$_5$ species added in ZnO materials does not significantly modify the grain-growth behavior of the samples. Figures 4(c$_1$)–(c$_3$) show that
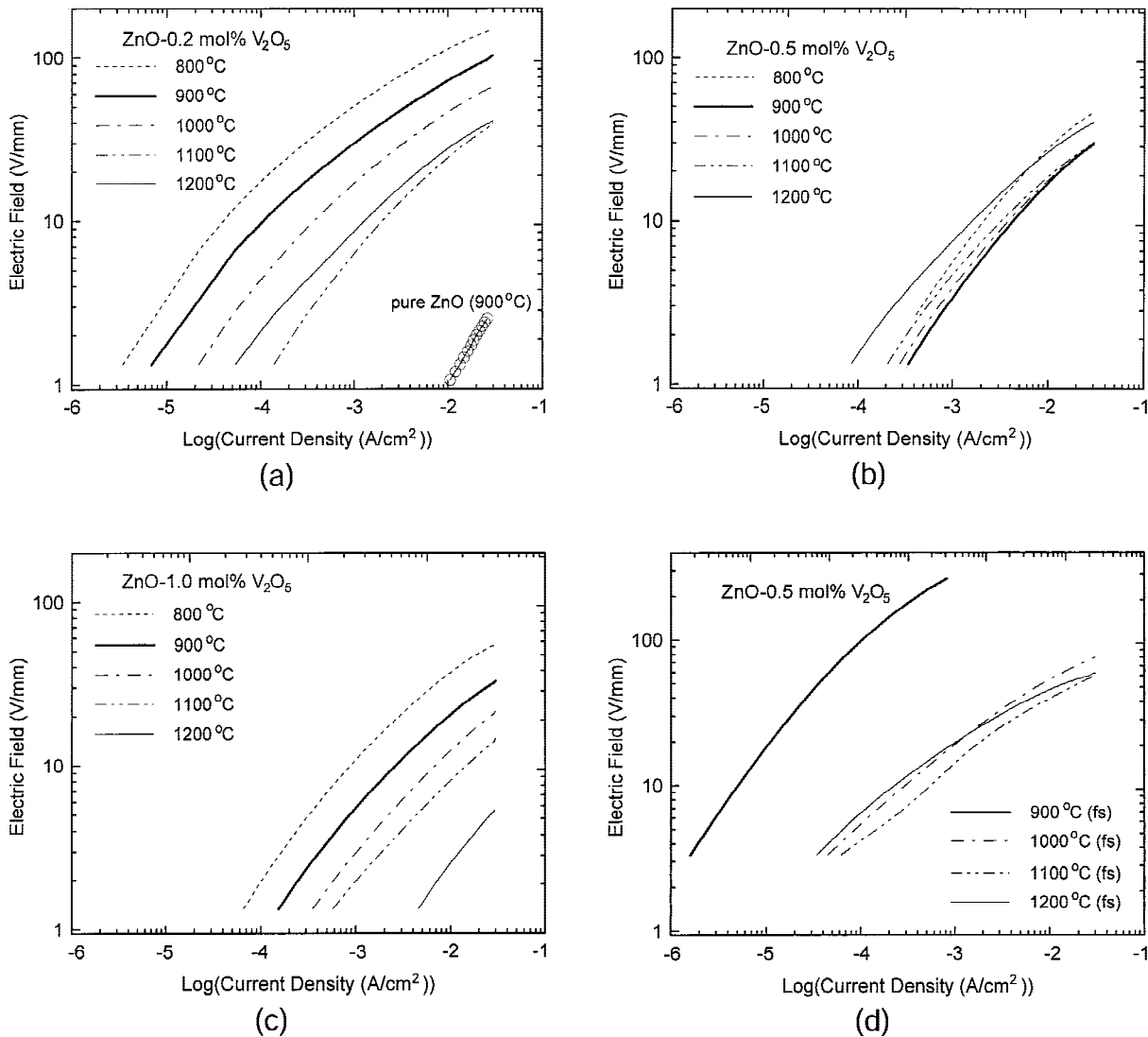
Fig. 6. Electric-field–current-density (E–J) characteristics of the (a) ZnO–0.2-mol%-V_2O_5, (b) ZnO–0.5-mol%-V_2O_5, and (c) ZnO–1.0-mol%-V_2O_5 materials microwave-sintered at 800°–1200°C for 10 min; Fig. 6(d) shows the E–J characteristics of the ZnO–0.5-mol%-V_2O_5 materials furnace-sintered at 900°–1200°C for 60 min.

grains of the ZnO–V_2O_5 materials already grow to a large size (15–18 μm) when the material is microwave-sintered at 900°C (10 min), whereas the grains of the pure ZnO materials sintered via the same conditions hardly grow. Moreover, the grain sizes of the samples increase monotonously as the sintering temperature and soaking time increase (Figs. 5(a) and (b), respectively). However, the SEM micrographs shown in Figs. 4(d) and (e) indicate that the material still requires a sufficient soaking period (i.e., 60 min at 900°C) or an adequate sintering temperature (i.e., 1000°C for 10 min) to develop a uniformly large-grained microstructure for ZnO–V_2O_5 materials. Trapped pores are observed in these samples, which implies that the grain-boundary mobility of the samples has surpassed the dragging force of the pores under these sintering conditions.

(2) Electrical Properties

The electrical properties of ZnO–V_2O_5 materials are characterized by their E–J behavior. Figures 6(a)–(c) show that the E–J properties are very sensitive to the processing parameters. The leakage of the current density is so pronounced in all the ZnO–V_2O_5 materials that there seems to be no nonlinear characteristics that are observable for all the samples. Figure 6(d) shows that the furnace-sintered samples also possess a large J_L value, except for the 900°C (60 min) sintered samples, which

are ascribed to the insufficient densification of these samples (cf. Fig. 2(a)). Such behavior can be ascribed to the fact that the grain-boundary phase, which is presumably the ZnO–V_2O_5 compound (i.e., $Zn_3(VO_4)_2$), reacts with the matrix very well, which results in an insufficient amount of surface states (N_s) and a small Schottky barrier height Φ_b along the grain-boundary regions.

To facilitate the comparison, the onset electric field E_0 is defined as the electric field that corresponds to a current density of 1 mA/cm² in the E–J curves and the leakage current density J_L is defined as the current density that passes through the samples under an applied field of 10 V/mm. Figures 6(a)–(c) show that, although the proportion of V_2O_5 additives included in the ZnO materials does not result in significantly different densification and grain-growth behavior of these materials (cf. Figs. 2(a) and 5(a)), it does markedly affect the E–J characteristics of the samples. The sintering temperature dependence of E_0 and J_L is shown in Figs. 7(a) and (b), respectively, which indicates that only the ZnO–0.5-mol%-V_2O_5 materials exhibit more-consistent E_0 and J_L parameters than the others; these parameters are $E_0 = 3.5$–7.6 V/mm and $J_L = 1.6 \times 10^{-3}$–3.8×10^{-3} A/cm².

The fact that the ZnO–0.5-mol%-V_2O_5 materials possess much more consistent electric properties is further shown as the
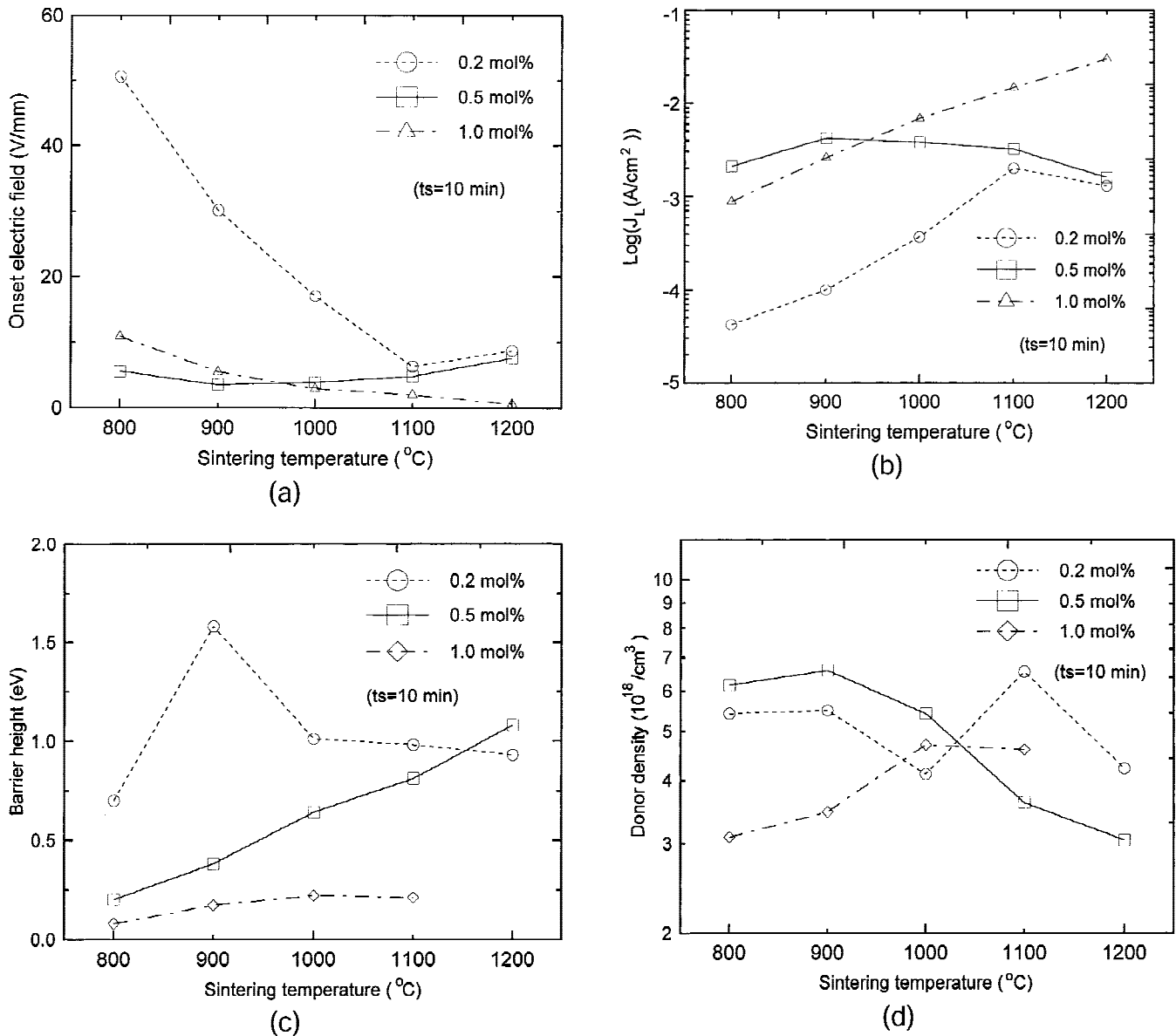
Fig. 7. Variation of the (a) onset electric field (E_0), (b) leakage current density (J_L), (c) barrier height (Φ_b), and (d) donor density (N_d) of ZnO–V₂O₅ materials with the sintering temperature.

sintering-temperature dependence of the barrier height Φ_b and the donor density N_d, in the ranges of 0.20–0.81 eV and 3.61 × 10^{18}–6.60 × 10^{18}/cm³, respectively (Figs. 7(c) and (d), respectively). Figures 8(a)–(c) indicate again that, for ZnO–0.5-mol%-V₂O₅ materials, the sintering time period (at a sintering temperature of 900°C) does not significantly alter the *E–J* characteristics and the related electrical parameters (i.e., E_0, J_L, Φ_b, and N_d), although it moderately changes the sintered density and the average grain size of the materials (cf. Figs. 2(b) and 5(b)).

The variation of the electrical properties of ZnO–V₂O₅ materials with the V₂O₅ content can be correlated very well with the corresponding granular structure. For the materials with a small V₂O₅ content (i.e., ZnO–0.2 mol% V₂O₅), the granular structure was fully developed only when they were sintered at sufficiently high temperature. The low-temperature-sintered materials still contain fine grains that are distributed among the large grains; this distribution results in large E_0 values, which are accompanied by low apparent J_L values. On the other hand, for the materials with a large V₂O₅ content (i.e., ZnO–1.0 mol% V₂O₅), high sintering temperatures induced pronounced V₂O₅ loss (cf. Fig. 3(b)), which reduces the value of E_0 and

increases the value of J_L. These results again reveal that the defect structure along the grain boundaries is another important characteristic that needs to be carefully controlled, in addition to the high sintered density and uniform microstructure, for the purpose of optimizing the electrical behavior of ZnO–V₂O₅ materials.

As described previously, although the V₂O₅ addition has markedly improved the densification and the grain-growth behavior of the ZnO materials, a substantial leakage current density remained, because of a lack of surface states along the grain boundaries for inducing Schottky barriers in these regions. To amend such a discrepancy, 0.3 mol% of Mn₃O₄ was included into the ZnO materials, in addition to the 0.5 mol% of V₂O₅, because the manganese species are expected to reside at the grain-boundary regions and act as electron traps to induce large potential barriers. The bold, solid curve in Fig. 8(a) shows the enormous improvement of the *E–J* behavior of ZnO materials due to Mn₃O₄ doping. The leakage current density is markedly suppressed to J_L = 2.4 × 10^{-6} A/cm², and the onset field is pronouncedly increased to E_0 = 97 V/mm, such that a nonlinear property with a high nonlinear coefficient (α = 23.5) is achieved. However, the details regarding how the Mn₃O₄
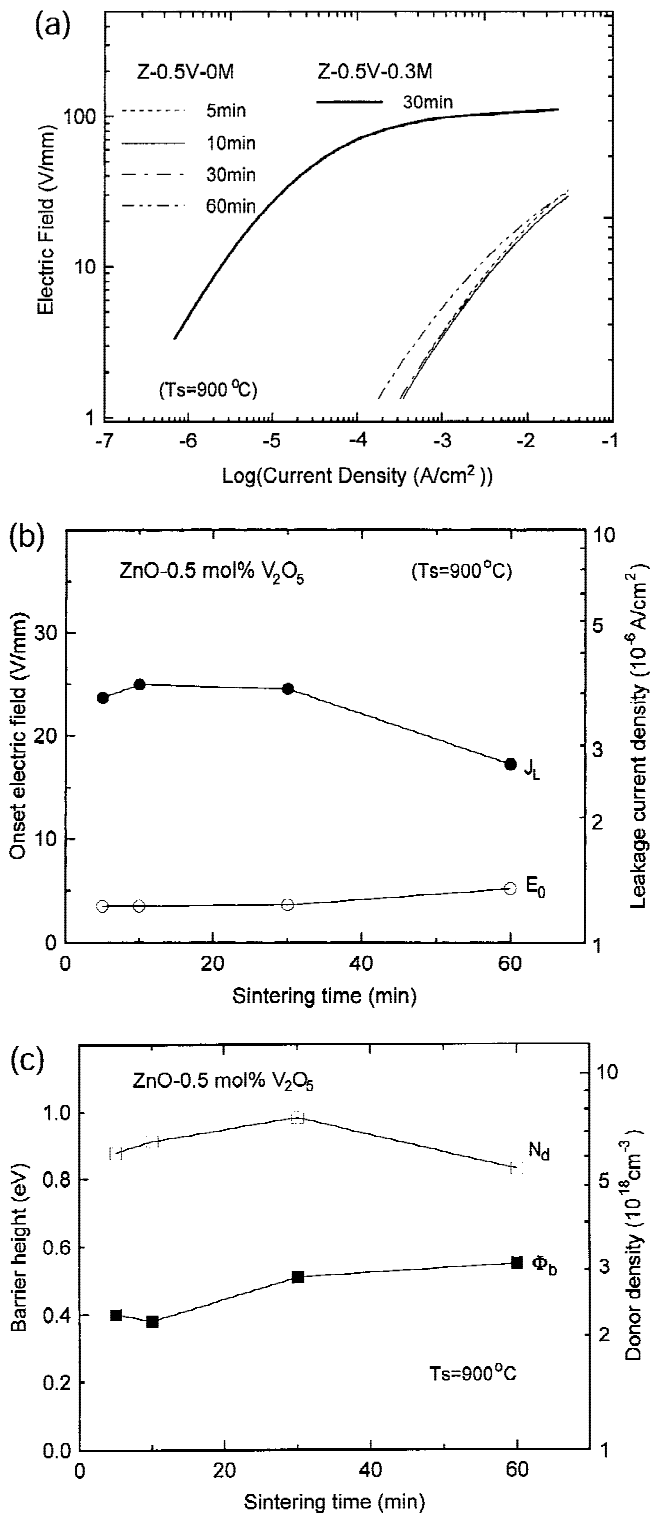
additives modify the characteristics of ZnO–V_2O_5 materials require additional study.

IV. Conclusions

The incorporation of V_2O_5 additives into ZnO materials pronouncedly enhances their densification and grain-growth rates. Densities as high as 97.9% of the theoretical density and grain sizes as large as 10 μm can be obtained via microwave sintering at temperatures as low as 800°C for 10 min. The sintering temperature and soaking time do not significantly affect the densification rate and the grain-growth behavior; however, they do markedly modify the electrical properties of these materials. The possible interaction between them has been discussed.

References

[1]M. Inada, "Crystal Phases on Non-ohmic Zinc Oxide Ceramics," *Jpn. J. Appl. Phys.*, **17** [1] 1–10 (1978).

[2]L. M. Levinson and H. R. Philipp, "Zinc Oxide Varistors—A Review," *Am. Ceram. Soc. Bull.*, **65** [4] 639–46 (1986).

[3]T. K. Gupta, "Application of Zinc Oxide Varistors," *J. Am. Ceram. Soc.*, **73** [7] 1817–40 (1990).

[4]K. Eda, A. Iga, and M. Matsuoka, "Degradation Mechanism of Non-ohmic Zinc Oxide Ceramics," *J. Appl. Phys.*, **51** [5] 2678–84 (1980).

[5]J. Erickson and B. Reich, "The High Power Metal-Oxide Varistor as a Vehicle and Aircraft Transient Suppresser," *IEEE Trans. Aerosp. Electron. Syst.*, **AES–12**, 104–108 (1976).

[6]L. M. Levinson and H. R. Philipp, "ZnO Varistors for Transient Protection," *IEEE Trans. Parts, Hybrids, Packag.*, **PHP–13**, 338–43 (1977).

[7]E. C. Sakshaug, J. S. Kresge, and S. A. Miske, "A New Concept in Station Arrestor Designs," *IEEE Trans. Power Appar. Syst.*, **PAS-96**, 647–56 (1977).

[8]R. Einzinger, "Metal Oxide Varistors," *Annu. Rev. Mater. Sci.*, **17**, 299–321 (1987).

[9]M. Matsuoka, "Nonohmic Properties of Zinc Oxide Ceramics," *Jpn. J. Appl. Phys.*, **10** [6] 736–46 (1972).

[10]K. Mukae, K. Tsuda, and I. Nagasawa, "Non-Ohmic Properties of ZnO–Rare Earth Metal Oxide–Co_3O_4 Ceramics," *Jpn. J. Appl. Phys.*, **16** [8] 1361–68 (1977).

[11]Y.-S. Lee and T.-Y. Tseng, "Phase Identification and Electrical Properties in ZnO–Glass Varistors," *J. Am. Ceram. Soc.*, **75** [6] 1636–40 (1992).

[12]K. Uematsu, A. Terada, T. Morimoto, N. Uchida, and K. Saito, "Direct Determination of Grain Growth Behavior in Zinc Oxide with Added Barium Oxide," *J. Am. Ceram. Soc.*, **72** [6] 1070–72 (1989).

[13]T. R. N. Kutty and N. Raghu, "ZnO-Based Voltage-Limiting Resistors with $MCoO_{3-x}$ (M ≡ Ba, Sr) as the Only Forming Additives," *Mater. Sci. Eng., B*, **B13**, 181–97 (1992).

[14]G. Calestani, L. Marshignani, and A. Montenero, "DC Conductivity of ZnO–V_2O_5 Glasses," *J. Non-Cryst. Solids*, **86**, 285–92 (1986).

[15]J. K. Tsai and T. B. Wu, "Non-Ohmic Characteristics of ZnO–V_2O_5 Ceramics," *J. Appl. Phys.*, **76** [8] 4817–22 (1994).

[16]J. K. Tsai and T. B. Wu, "Microstructures and Nonohmic Properties of ZnO–V_2O_5 Ceramics," *Jpn. J. Appl. Phys.*, **34** [12] 6452–57 (1995).

[17]W. H. Sutton, "Microwave Processing of Ceramic Materials," *Am. Ceram. Soc. Bull.*, **68** [2] 376–86 (1989).

[18]M. A. Janney, C. L. Calhoum, and H. D. Kimery, "Microwave Sintering of Solid Oxide Fuel Cell Materials: I. Zirconia–8 mol% Yttria," *J. Am. Ceram. Soc.*, **75** [2] 341–46 (1992).

[19]H. Y. Chang, K. S. Liu, and I. N. Lin, "Electrical Characteristics of $(Sr_{0.2}Ba_{0.8})TiO_3$ Positive Temperature Coefficient of Resistivity Materials Prepared by Microwave Sintering," *J. Appl. Phys.*, **77** [11] 1–5 (1995).

[20]C. S. Chen, C. T. Kuo, and I. N. Lin, "Electrical Properties of ZnO Varistors Prepared by Microwave Sintering Process," *Jpn. J. Appl. Phys.*, **35** [9] 4696–703 (1996).

[21]M. I. Mendelson, "Average Grain Size in Polycrystalline Ceramics," *J. Am. Ceram. Soc.*, **52** [8] 443–46 (1969).

[22]K. Mukae, K. Tsuda, and I. Nagasawa, "Capacitance-vs-Voltage Characteristics of ZnO Varistors," *J. Appl. Phys.*, **50** [6] 4475–76 (1979). □

Fig. 8. Variation of (a) the *E–J* characteristics, (b) the onset electric field (E_0) and the leakage current density (J_L), and (c) the barrier height (Φ_b) and donor density (N_d) with the soaking time (5–60 min) of the ZnO–0.5-mol%-V_2O_5 (Z-0.5V-0M) materials microwave-sintered at 900°C (the bold curve in Fig. 8(a) shows the modification on the *E–J* curve due to the Mn_3O_4 addition, Z-0.5V-0.3M).